Ann Nucl Med (2008) 22:191–200
DOI 10.1007/s12149-007-0099-7

ORIGINAL ARTICLE

Influence of mild hyperglycemia on cerebral FDG distribution patterns calculated by statistical parametric mapping

Keiichi Kawasaki · Kenji Ishii · Yoko Saito
Keiichi Oda · Yuichi Kimura · Kiichi Ishiwata

Received: 2 October 2007 / Accepted: 29 November 2007

Abstract
Objective In clinical cerebral 2-[^{18}F]fluoro-2-deoxy-D-glucose positron emission tomography (FDG-PET) studies, we sometimes encounter hyperglycemic patients with diabetes mellitus or patients who have not adhered to the fasting requirement. The objective of this study was to investigate the influence of mild hyperglycemia (plasma glucose range 110–160 mg/dl) on the cerebral FDG distribution patterns calculated by statistical parametric mapping (SPM).
Methods We studied 19 healthy subjects (mean age 66.2 years). First, all the subjects underwent FDG-PET scans in the fasting condition. Then, 9 of the 19 subjects (mean age 64.3 years) underwent the second FDG-PET scans in the mild hyperglycemic condition. The alterations in the FDG-PET scans were investigated using SPM- and region of interest (ROI)-based analyses. We used three reference regions: (1) SPM global brain (SPMgb) used for SPM global mean calculation, (2) the gray and white matter region computed from magnetic resonance image (MRIgw), and (3) the cerebellar cortex (Cbll).
Results The FDG uptake calculated as the standardized uptake value (average) in SPMgb, MRIgw, and Cbll regions in the mild hyperglycemic condition was 42.7%, 41.3%, and 40.0%, respectively, of that observed in the fasting condition. In SPM analysis, the mild hyperglycemia was found to affect the cerebral distribution patterns of FDG. The FDG uptake was relatively decreased in the gray matter, mainly in the frontal, temporal, and parietal association cortices, posterior cingulate, and precuneus in both SPMgb- and MRIgw-reference-based analyses. When Cbll was adopted as the reference region, those decrease patterns disappeared. The FDG uptake was relatively increased in the white matter, mainly in the centrum semiovale in all the reference-based analyses.
Conclusions It is noteworthy that the FDG distribution patterns were altered under mild hyperglycemia in SPM analysis. The decreased uptake patterns in SPMgb- (SPM default) and MRIgw-reference-based analyses resembled those observed in Alzheimer's disease. Under mild hyperglycemia, we can recommend Cbll as the reference region to detect decreased uptake patterns. We should pay special attention to controlling the diet condition, monitoring hyperglycemia, and optimizing the reference region in SPM analysis, particularly in the diagnosis of early Alzheimer's disease in clinical FDG-PET.

Keywords FDG-PET · Mild hyperglycemia · Distribution pattern · Statistical parametric mapping · Alzheimer's disease

Introduction

Cerebral 2-[^{18}F]fluoro-2-deoxy-D-glucose positron emission tomography (FDG-PET) examinations are widely used for the diagnosis of neurological disorders such as dementia, epilepsy, and tumors. A high plasma glucose level and diet-enhanced FDG uptake by extra-brain tissues decrease the FDG uptake in the brain and reduce the quality of brain images [1, 2]. So the examinations

K. Kawasaki (✉) · K. Ishii · Y. Saito · K. Oda · Y. Kimura · K. Ishiwata
Positron Medical Center, Tokyo Metropolitan Institute of Gerontology, 1-1 Naka-cho, Itabashi-ku, Tokyo 173-0022, Japan
e-mail: kawasaki@pet.tmig.or.jp

are usually carried out after a 4–6-h fast to give a low plasma glucose concentration. However, FDG-PET is sometimes carried out in hyperglycemic patients with diabetes mellitus, or in patients who have not adhered to the fasting requirement. Nevertheless, in most cases, the glucose level is still less than the criterion of hyperglycemia (plasma glucose > 160 mg/dl) as described in the "European Association of Nuclear Medicine Procedure Guidelines for Brain Imaging using [^{18}F]FDG" [2]. In such mild hyperglycemic cases, it is usually assumed that the FDG distribution pattern in the brain in the fasting condition is maintained regardless of plasma glucose levels.

In recent years, clinical examinations require the detection of subtle abnormalities of regional cerebral FDG uptake in patients with neurological disorders such as early Alzheimer's disease and refractory focal epilepsy. Usually, static (semi-quantitative) images of FDG are used, and when data from age-matched normal controls are available, the data from each patient are evaluated by statistical approaches such as statistical parametric mapping (SPM) [3] and three-dimensional (3D) stereotactic surface projection (3D-SSP) techniques [4].

In the course of the SPM analysis in the FDG-PET studies, we have encountered patients who had not fasted but whose plasma glucose level was no more than 160 mg/dl. However, the results of the SPM analysis sometimes showed abnormalities different from the clinical presentation.

With regard to the relationship between cerebral glucose metabolism and the plasma glucose level, Hasselbalch et al. [6] measured the global cerebral metabolic rate of glucose (CMRglc) and regional CMRglc (rCMRglc) on the basis of the Sokoloff model [5] in normoglycemic control condition (plasma glucose 97 mg/dl) and in an acute hyperglycemic condition (270 mg/dl) in six normal subjects. They reported that during acute hyperglycemia, when compared with the normoglycemia, with the exception of a significant increase (42%) in the white matter in the centrum semiovale, the global CMRglc and rCMRglc in the cortical and subcortical gray matter regions did not change. However, if a significant increase occurs unexpectedly in the white matter in the centrum semiovale during hyperglycemia, as demonstrated by Hasselbalch et al. [6], the subjects whose plasma glucose level is not controlled to the fasting level may be erroneously diagnosed by the statistical approaches. Therefore, it is necessary to investigate whether the plasma glucose levels alter the regional cerebral FDG uptake, thereby possibly influencing the FDG distribution patterns obtained by using the statistical approaches.

In the present study, we focused on the glucose levels less than the aforementioned criterion of hyperglycemia (>160 mg/dl) [2]. As a fasting glucose level from 70 mg/dl to 109 mg/dl in plasma is generally considered to be normal, we defined the plasma glucose level from 110 mg/dl to 160 mg/dl as mild hyperglycemia.

The objective of this study was to investigate the influence of plasma glucose levels within the mild hyperglycemia on the cerebral FDG distribution patterns, particularly the patterns obtained by using SPM analysis.

Materials and methods

Subjects and conditions

We studied 19 healthy subjects (6 men and 13 women) with a mean age of 66.2 years (range 48–80 years). All the subjects fulfilled the following criteria: (1) no history of diabetes mellitus, neurological or psychiatric disorders, head trauma, drug abuse, alcoholism, hypertension, or cardiac disease, (2) no medication, (3) found to be normal on physical and neurological examinations, (4) Mini-Mental State Examination score = 30, and (5) found to be normal on anatomical magnetic resonance imaging (MRI), i.e., 3D-MRI (described below) and T2-weighted MRI. This study was approved by the institutional Ethics Committee. A written informed consent was obtained from all the subjects before the study.

First all the subjects underwent FDG-PET scanning in the fasting condition (after >5-h fasting). Then, within 1 month, 9 of the 19 subjects (2 men and 7 women, mean age 64.3 years, range 48–80 years) underwent a second FDG-PET scanning in the mild hyperglycemic condition in which each subject first consumed a normal lunch 2–2.5 h prior to the FDG injection and was then orally administered 50 g glucose (TRELAN-G50, 150 ml; Ajinomoto Pharma, Tokyo, Japan) 30 min prior to the FDG injection. At PET measurement 1–2 ml of venous blood samples were drawn twice immediately prior to the intravenous FDG injection and 30 min following the injection (t = 0 min and 30 min, respectively), and the plasma glucose concentration was measured. The paired comparison between the fasting and mild hyperglycemic conditions was done using the data obtained from the 9 subjects scanned twice, and the comparisons between one scan in the fasting or hyperglycemic condition and the normal database were done between the data obtained from the 9 subjects and the data of the 19 subjects in the fasting condition.

Image acquisition

For all subjects, the 3D-MRI images with T1-weighted contrast were obtained with a 1.5-T Sigma Horizon scanner (GE, Milwaukee, WI, USA) using the following imaging parameters: matrix size 256 × 256 × 124 and voxel size 0.9375 × 0.9375 × 1.3 mm. The images were obtained using the 3D spoiled gradient echo protocol (TR/TE = 9.2 ms/2.0 ms) before the first FDG-PET scan.

FDG images were obtained with a PET scanner (SET 2400W; Shimadzu, Kyoto, Japan) in the 3D mode [image resolution: transverse full width at half-maximum (FWHM) = 4.4 mm, axial FWHM = 6.5 mm]. Forty-five minutes following the intravenous injection of FDG (130.4 ± 15.0 MBq), a 6-min emission scan was collected to create images with the following parameters: matrix size 128 × 128 × 50 and voxel size 2 × 2 × 3.125 mm. The attenuation was corrected by a transmission scan using a ^{68}Ga/^{68}Ge source. During the tracer-accumulation phase, the subjects remained supine, quiet, and motionless in a dimly lit and quiet (except for air-conditioner noise) room with their eyes open and ears unoccluded.

Image processing

Image processing and data analysis were performed using SPM2 (Functional Imaging Laboratory, London, UK) implemented on MATLAB (The MathWorks, Natick, MA, USA) and Dr. View (AJS, Tokyo, Japan). The tasks performed by SPM2 were MRI/PET coregistration, spatial normalization, spatial smoothing, MRI segmentation, normalization for reference region, and SPM analysis. The tasks performed by Dr. View were image masking and region of interest (ROI) analysis. All FDG images were spatially normalized and resampled (XYZ matrix 79 × 95 × 80 and voxel size 2 × 2 × 2 mm) using the FDG template which was created from the FDG images of 15 physically and psychiatrically healthy subjects (mean age 33.3 years, range 20–49 years) in accordance with a method described elsewhere [7]. Each 3D-MRI image was coregistered to the corresponding FDG image in the fasting condition and normalized to the FDG template using the parameters obtained from the spatial normalization of the corresponding FDG images.

To investigate alterations of regional FDG uptake and FDG distribution patterns, we used three kinds of image reference regions termed as SPMgb, MRIgw, and Cbll (Fig. 1). SPMgb (Fig. 1b) indicates the SPM global brain region used for the calculation of global mean in default in SPM program. SPMgb is defined implicitly in each image by using a two-step process: first the overall mean is computed, and then voxels measuring less than the quotient of the mean divided by 8 are deemed extracranial and are masked out. Thus, SPMgb is uniquely defined image-by-image. The global mean is then recomputed on the remaining voxels. MRIgw (Fig. 1c) indicates an MRI-based gray and white matter region computed using the segmentation function of SPM program and is defined for each subject separately. Cbll

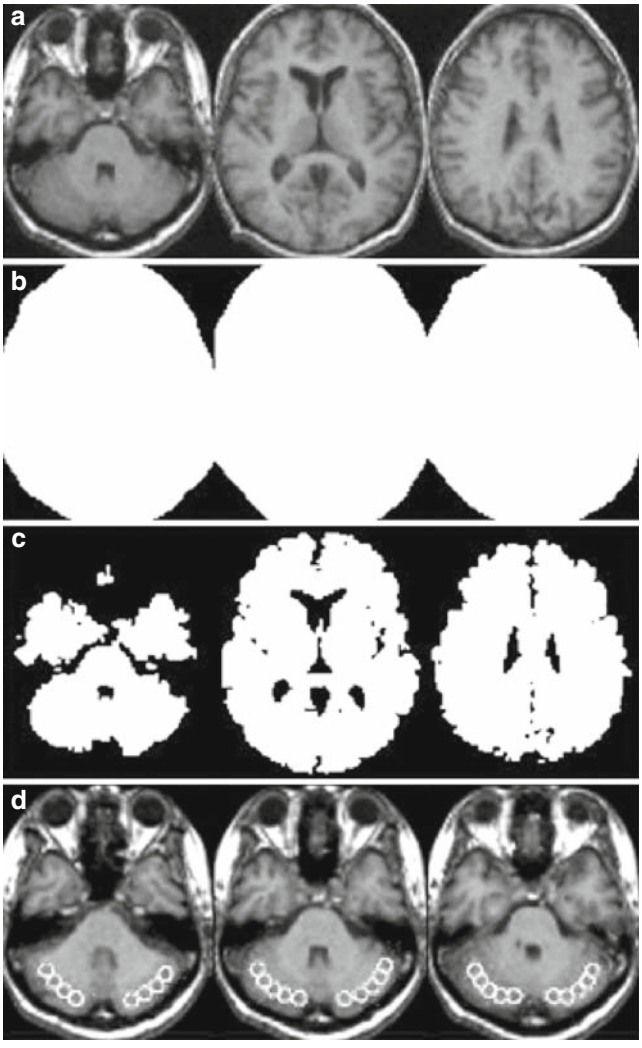

Fig. 1 An example of the brain regions investigated. **a** The space normalized 3D-magnetic resonance imaging (MRI) image of a subject. **b** Statistical parametric mapping global brain (SPMgb) computed from the 2-[^{18}F]fluoro-2-deoxy-D-glucose positron emission tomography (FDG-PET) image of the subject in the fasting condition in default in SPM program (smoothed using a Gaussian filter with a 16-mm full width at half-maximum). SPMgb in the mild hyperglycemic condition was nearly equal to that in the fasting condition (not shown). **c** MRIgw consisting of the gray and white matter regions computed from the 3D-MRI image of the subject using SPM segmentation function. **d** Cerebellar cortex [Cbll, region of interest (ROI) on cerebellar cortex] consisting of 48 circles 10 mm in diameter on five continuous slices

(Fig. 1d) indicates the ROI on the cerebellar cortex common to all spatially normalized images. It is noted that the MRIgw includes gray and white matter regions, whereas the SPMgb contains the entire intracranial contents including cerebrospinal fluid and orbit regions.

The subject mean of SPMgb, MRIgw, and Cbll of each FDG image after spatial normalization was normalized to be 50 to create SPMgb- MRIgw-, and Cbll-reference-based images.

Data analysis

Regional uptake of the FDG

The FDG uptake in SPMgb, MRIgw, and Cbll in each scan for each subject scanned twice was expressed as the standardized uptake value [SUV, body weight (g) × tissue concentration (Bq/ml)/total injected dose (Bq). We performed the paired Wilcoxon t test comparing the FDG uptake (SUV) in the three reference regions between the two scans; $P < 0.01$ was considered to be significant.

SPM-based analysis of the FDG uptake

We performed three global normalization processes on the basis of SPMgb-, MRIgw-, and Cbll-reference-based images. Those images were smoothed using a Gaussian filter with a 16-mm FWHM to increase the sensitivity and then we calculated the statistical parametric maps of the paired t test between the first and second scans of the subjects scanned twice by the "Population main effect: 2 cond's, 1 scan/cond" of SPM analysis design type ($P < 0.001$, uncorrected, extent threshold $k = 300$ voxels). We also calculated the statistical maps using "Compare-populations: 1 scan/subject (Ancova)" with age as a covariate between each scan in the fasting or mild hyperglycemic condition of the 9 subjects and the scans in the fasting condition of the other 18 of the 19 subjects (1 of the 19 subjects under comparison was excluded) using it as the normal database ($P < 0.01$, uncorrected, extent threshold $k = 300$ voxels).

ROI-based analysis of the FDG uptake

In the subjects scanned twice, the ROIs common to all normalized images were placed on the Cbll, centrum semiovale, and the frontal, temporal, and parietal cortices, and posterior cingulate/precuneus. The ROIs of the Cbll, centrum semiovale, and the frontal, temporal, and parietal cortices, and posterior cingulate/precuneus consisted of 48 circles 10 mm in diameter on 5 continuous slices, 26 on 5, 116 on 16, 116 on 17, 50 on 7, and 46 on 17, respectively. The relative FDG uptake in the ROIs was calculated in SPMgb-, MRIgw-, and Cbll-reference-based images without smoothing. For the ROI-based statistical analysis, the paired Wilcoxon t test was performed for each of the six ROIs between two scans; $P < 0.05$ with Bonferroni correction (total number of comparisons = 6, new alpha level = 0.0083) was considered to be significant.

Results

Fasting and mild hyperglycemic conditions

The plasma glucose concentration was significantly increased in the mild hyperglycemic condition: fasting scan (19 subjects), 91.7 ± 4.6 mg/dl at $t = 0$ min and 90.8 ± 5.5 mg/dl at $t = 30$ min; fasting scan (9 subjects scanned twice within 19 subjects), 90.0 ± 4.4 mg/dl at $t = 0$ min and 90.9 ± 6.9 mg/dl at $t = 30$ min; and mild hyperglycemic scan (9 subjects), 136.1 ± 10.5 mg/dl at $t = 0$ min, 138.1 ± 14.0 mg/dl at $t = 30$ min.

Three image reference regions and the FDG uptake

Figure 1 represents the space normalized 3D-MRI image of a subject and the three defined image reference regions (SPMgb, MRIgw, and Cbll). The SPMgb regions in both the fasting and mild hyperglycemic conditions were nearly equal.

The FDG uptake (SUV) in the three reference regions decreased greatly in the mild hyperglycemic condition ($P < 0.01$, Fig. 2). The SUV values in the SPMgb, MRIgw, and Cbll in the mild hyperglycemic condition were 42.7%, 41.3%, and 40.0%, respectively, of those observed in the fasting condition.

Paired comparison between the fasting and mild hyperglycemic conditions

First, the paired t test between the fasting and mild hyperglycemic conditions was performed by SPM, and the results are shown in Fig. 3 ($P < 0.001$, uncorrected, $k = 300$). In the contrast "uptake in the mild hyperglycemic condition < uptake in the fasting condition (uptake in M.hygl < uptake in Fasting)", the uptake in the gray matter and cerebellar cortex regions greatly decreased in SPMgb-reference-based analysis (Fig. 3a), and clear decreases were detected in the frontal, temporal, and parietal cortices, posterior cingulate, and precuneus in MRIgw-reference-based analysis (Fig. 3b). However, no decreased uptake pattern was detected in Cbll-reference-based analysis (not shown). In the contrast "uptake in

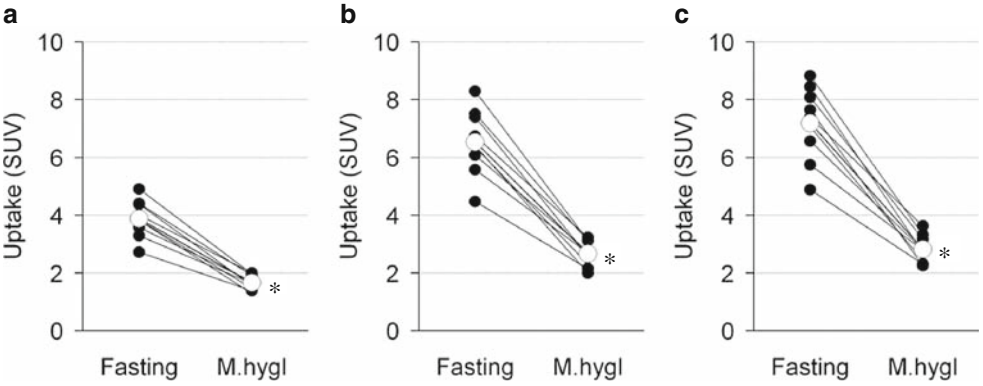

Fig. 2 FDG uptake (standardized uptake value) in SPMgb (**a**), MRIgw (**b**), and Cbll (**c**), respectively. The uptake was compared in the nine subjects scanned twice in the fasting and mild hyperglycemic (M.hygl) conditions. *Solid circles* represent individual subjects, and *open circles* represent the average ($n = 9$). *$P < 0.01$ (paired Wilcoxon t test)

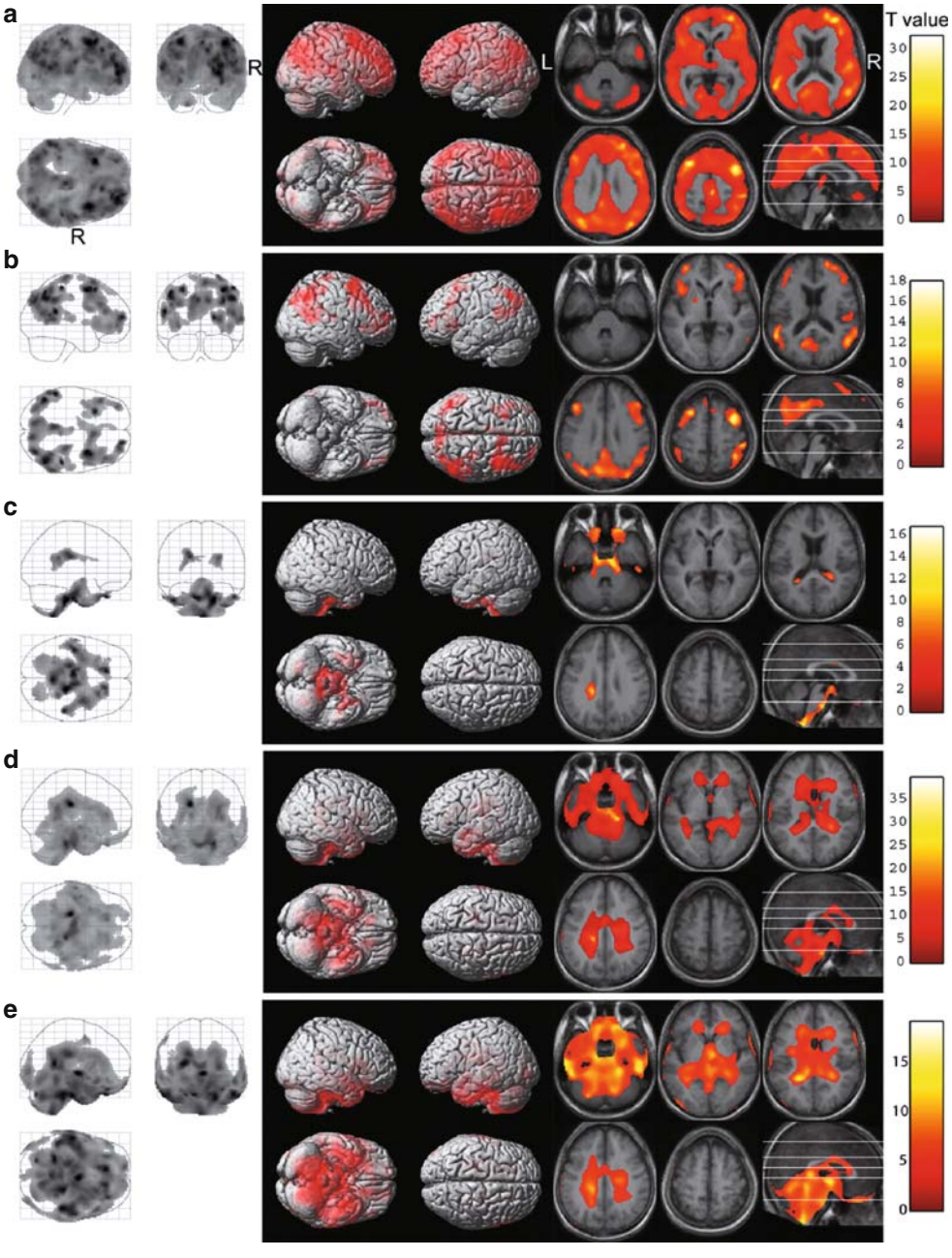

Fig. 3 SPM paired t tests "uptake in M.hygl < uptake in Fasting" in SPMgb- (**a**) and MRIgw- (**b**) reference-based analyses, and "uptake in M. hygl > uptake in Fasting" in SPMgb- (**c**), MRIgw- (**d**), and Cbll- (**e**) reference-based analyses. No decreased uptake pattern was detected in the mild hyperglycemic condition in Cbll-reference-based analysis (not shown). The SPM paired t tests were performed in the nine subjects scanned twice in the fasting and mild hyperglycemic conditions ($P < 0.001$, uncorrected; $k = 300$)

the mild hyperglycemic condition > uptake in the Fasting condition (uptake in M.hygl > uptake in Fasting)", the uptake increased in the centrum semiovale and cerebrospinal fluid regions in SPMgb-reference-based analysis (Fig. 3c), whereas significant increases were revealed in the white matter, cerebellar medullary substance, and cerebrospinal fluid regions in MRIgw- and Cbll-reference-based analyses (Fig. 3d, e).

Second, ROI-based analysis was performed for the FDG uptake in the six regions in both the fasting and mild hyperglycemic conditions in SPMgb-, MRIgw-, and Cbll-reference-based images. In the mild hyperglycemic condition, the uptake significantly decreased in the frontal (9.9%), temporal (7.6%), and parietal (9.2%) cortices, posterior cingulate/precuneus (9.9%), and Cbll (7.8%) in SPMgb-reference-based images (Fig. 4a), and in the frontal (5.6%) and temporal (3.2%) cortices, and posterior cingulate/precuneus (5.4%) in MRIgw-reference-based images (all $P < 0.05$, Fig. 4b), but no decreased uptake ROI was revealed in Cbll-reference-based images (Fig. 4c). On the other hand, the uptake significantly increased in the centrum semiovale: 10.8%, 16.1%, and 20.1% in SPMgb- (Fig. 4a), MRIgw- (Fig. 4b), and Cbll- (Fig. 4c) reference-based images, respectively (all $P < 0.05$).

Comparison between one scan in the fasting or mild hyperglycemic condition and the normal database

"Compare-populations: 1 scan/subject (Ancova)" with age as a covariate between each scan in the fasting or mild hyperglycemic condition of the 9 subjects and the scans in the fasting condition of the other 18 of the 19 subjects was performed by SPM, and the results in the contrast "uptake of one scan < uptake of the normal database" are shown on the sagittal projection in Fig. 5 ($P < 0.01$, uncorrected, $k = 300$). In the fasting condition, no notably decreased uptake pattern in common with nine subjects was detected in SPMgb-reference-based analysis (Fig. 5a). The spots observed in subjects 1, 4, 6, 7, and 9 were considered to be derived from individual morphological deviations that were not completely fitted to the FDG-PET template when compared with MRI images of each subject. In the mild hyperglycemic condition, significant decreases were observed in the association cortices such as frontal, temporal, and parietal cortices, posterior cingulate, and precuneus in SPMgb-reference-based analysis (Fig. 5b). The regions showing decreased uptake were greatly reduced in MRIgw-reference-based analysis, but the decreases were observed in the association cortices, posterior cingulate, and precuneus in some subjects (Fig. 5c). However, no decreased uptake patterns in any subjects were revealed in Cbll-reference-based analysis (not shown).

The results in the contrast "uptake of one scan > uptake of the normal database" were as follows (figures not shown). In the fasting condition, no notably increased uptake in common with nine subjects was detected. In the mild hyperglycemic condition, slight increases were observed in the white matter, cerebellar medullary substance, and cerebrospinal fluid regions in SPMgb-reference-based analysis in some subjects. The regions showing increased uptake spread widely in MRIgw- and Cbll-reference-based analyses.

Discussion

It is well known that a high plasma glucose concentration globally reduces FDG uptake in the brain [1, 2]. In this study, we confirmed that mild hyperglycemia (plasma glucose levels from 110 mg/dl to 160 mg/dl) decreased the FDG uptake in the SPMgb, MRIgw, and Cbll regions to 42.7%, 41.3%, and 40.0% of that in the fasting condition, respectively (Fig. 2).

Regarding the FDG distribution patterns calculated by SPM, we obtained the following findings. The mild hyperglycemia relatively decreased the FDG uptake in the gray matter in both SPMgb- and MRIgw-reference-based analyses (Figs. 3a, b, 4b, c). It should be noted that the regions showing relatively decreased uptake were the frontal, temporal, and parietal association cortices, posterior cingulate, and precuneus. It is well recognized that rCMRglc decreases in these association cortices are observed in Alzheimer's disease [8–12], and the decrease in the posterior cingulate and precuneus is considered to be an early sign of this disorder [13, 14]. Therefore, these findings demonstrate the possibility that SPMgb- or MRIgw-reference-based SPM analysis in FDG-PET could erroneously diagnose normal subjects whose plasma glucose levels were not below 110 mg/dl as patients with the early stages of Alzheimer's disease. However, the mild hyperglycemia did not reveal any decreases of FDG uptake in Cbll-reference-based analysis. Considering this result, we can recommend Cbll-reference-based analysis in the diagnosis of early Alzheimer's disease in the mild hyperglycemic condition. On the other hand, when we calculated the uptake increase regions in the mild hyperglycemic condition, the increases in the white matter, cerebellar medullary substance, and cerebrospinal fluid regions were detected, strongly, in MRIgw- and Cbll-reference-based analyses (Fig. 3c–e). Then, we realized that it would be difficult to detect increased uptake patterns characteristic of some degenerative diseases in SPM analysis in the mild hyperglycemic condition.

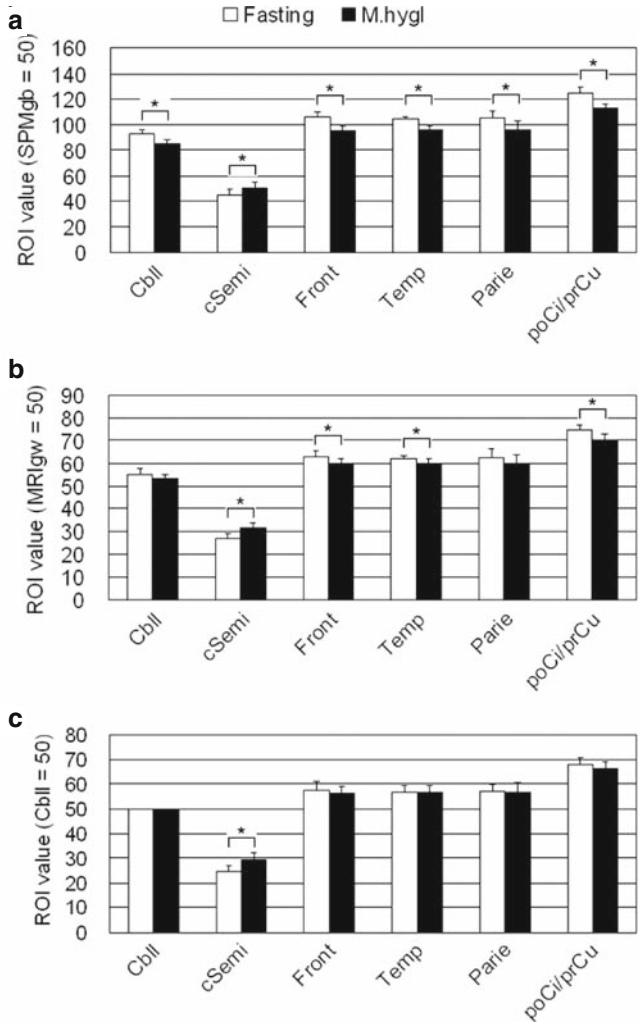

Fig. 4 Relative regional FDG uptake in the brain in the fasting and mild hyperglycemic (M.hygl) conditions in the SPMgb- (**a**), MRIgw- (**b**), and Cbll- (**c**) reference-based images. *Cbll* cerebellar cortex, *cSemi* centrum semiovale, *Front* frontal cortex, *Temp* temporal cortex, *Parie* parietal cortex, and *poCi/prCu* posterior cingulate/precuneus. The region of interest (ROI) values are shown as mean and SD ($n = 9$). *$P < 0.05$ (paired Wilcoxon t test with Bonferroni correction)

The most notable factor making a difference in the SPM results (T values) depending on the reference regions would be the difference in the relative amount of gray matter included in each reference region (Fig. 1). This is because the FDG uptake alterations induced by mild hyperglycemia in the gray matter and other regions were toward opposite directions: a decrease in the gray matter, but an increase in the white matter and extracerebral tissues (Figs. 3, 4).

Regarding the test–retest reproducibility of FDG-PET, several groups have confirmed that the global CMRglc and rCMRglc were reproducible, and the relative rCMRglc was more stable than the rCMRglc in the fasting condition within and among normal subjects with ages ranging from 23 years to 38 years in an ROI-based analysis [15–18]. Prior to the present study, we also confirmed the reproducibility of FDG-PET in the fasting condition within and among aged healthy subjects with ages ranging from 48 years to 80 years by the same method used in the present SPM-based analysis (unpublished data). The intrasubject test was done within 10 subjects, and the intersubject test was done between the 10 subjects and 9 subjects. The paired t test for the comparison within subjects and the two-sample t test for the comparison among subjects by SPM did not reveal variations in any of the normalization processes based on SPMgb, MRIgw, or Cbll ($P < 0.001$, uncorrected, $k = 300$).

In the FDG-PET study conducted by Hasselbalch et al. [6], the plasma glucose level (270 mg/dl) during hyperglycemia was approximately twice as high as that observed in the mild hyperglycemic condition (137 mg/dl) of the present study. In addition, the plasma glucose levels in their study were clamped by a constant infusion of somatostatin and insulin and variable intravenous infusions of 20% glucose. In terms of the glucose intake method, extrinsic factors of the brain (intravenous and passive intake of nutrients) were reflected in their study, but intrinsic factors (oral and spontaneous intake of nutrients) were reflected in our study. They reported that no global or regional difference in CMRglc was apparent during hyperglycemia, except for a significant increase in white matter in the centrum semiovale (42%). It is noted that Hasselbalch et al. [6] compared the quantitative CMRglc values in normal and hyperglycemic conditions, whereas we studied differences in distribution patterns by the SMP- and ROI-based analyses using relative data (Figs. 3, 4, 5). When we calculated the relative rCMRglc values normalized by the global CMRglc using the values reported in their article, the percentage rates of the relative decrease were 7.4% in the frontal cortex, 4.1% in the temporal cortex, and 8.4% in the parietal cortex, and the rate of the relative increase was calculated to be 30.6% in the centrum semiovale. It is speculated that their high glucose level induced much higher uptake in the centrum semiovale as compared with the present study: 30.6% versus 20.1% (Cbll-reference-based study, Fig. 4c). As the reason why they found no regional difference in rCMRglc values except for the significant increase in the centrum semiovale, we suspect that they compared quantitative CMRglc values between two conditions using ROI-based analysis. It would be of great interest if the paired t test of SPM using their CMRglc data provided results similar to ours in Fig. 3.

The following possible reasons can explain the phenomenon that FDG distribution patterns in the brain

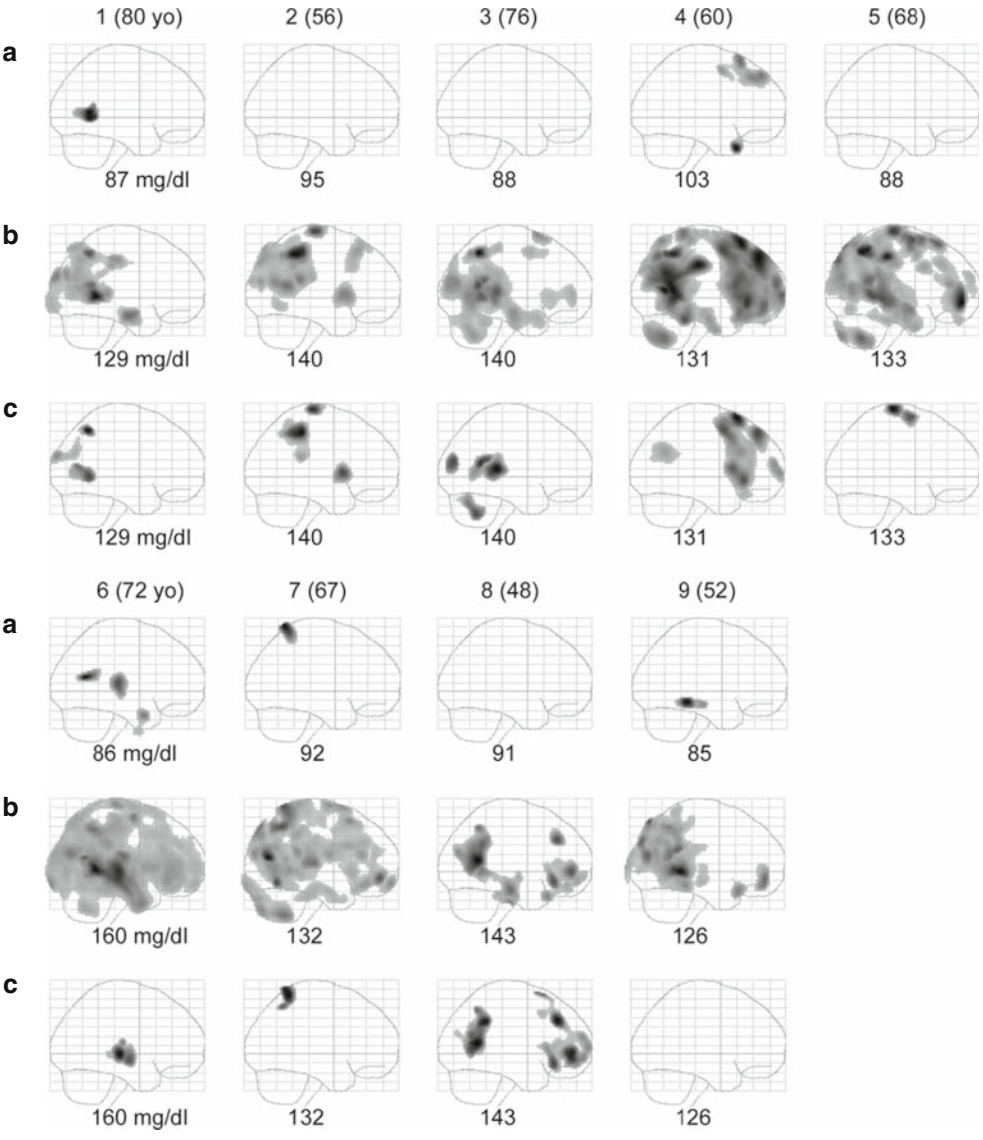

Fig. 5 SPM "Compare-populations: 1 scan/subject (Ancova)" with age as a covariate between each scan of the 9 subjects in the fasting or mild hyperglycemic condition and the scans of the other 18 of the 19 subjects in the fasting condition ($P < 0.01$, uncorrected, $k = 300$): "uptake of one scan in Fasting < uptake of the normal database" in SPMgb-reference-based analysis (**a**), and "uptake of one scan in M.hygl < uptake of the normal database" in SPMgb- (**b**) and MRIgw-reference-based analyses (**c**). No decreased uptake patterns in any subjects were revealed in Cbll-reference-based analysis (not shown). Subject numbers and ages in *parentheses* are presented on the top of three images of each subject and plasma glucose concentration (average) is presented at the bottom of each image

were regionally altered in the fasting and mild hyperglycemic conditions. (1) Difference in the cytoarchitecture that may cause a regional difference in the expression of glucose transporters and hexokinase and in turn may cause a regional difference in the lumped constant [5, 19, 20]. (2) The influence of the endocrine system, autonomic nervous system, psychological factors, or plasma glucose level related to the dietary condition may affect the regional cerebral function [6, 21, 22]. Regarding reason (1), the glucose transporter subtype 1 (GLUT1) is ubiquitously expressed in the brain, and the blood–brain barrier is a major site of its expression [23, 24]; on the other hand, the glucose transporter subtype 3 (GLUT3)—the predominant neuronal glucose transporter—is expressed in neurons [24, 25]. Asano et al. [26] had expressed the GLUT3 protein in Chinese hamster ovary (CHO) cells by the transfection of its cDNA by using an expression vector and compared its characteristics with those of the GLUT1 protein. A kinetic analysis revealed that the Michaelis constant (K_m) value of the GLUT3 protein for 3-*O*-methylglucose uptake in CHO cells was approximately 35% of that of GLUT1, whereas the K_m value of the GLUT3 protein for 2-deoxyglucose uptake was very similar to that of the GLUT1 protein. These data suggest the possibility that the regional differences in the expression ratios of GLUT1 and GLUT3 [27] and the heterogeneity of these transporters affect the FDG distribution patterns under mild hyperglycemia.

An epidemiological survey in Japan demonstrated that the frequency of diabetes mellitus diagnosed by the glucose tolerance test increased with age, with the frequency reaching 10–15% in elderly people aged 60 years or older with a high incidence of dementia [28]. In our institute these subjects sometimes undergo FDG-

PET for elucidating suspicious dementia, but the mild hyperglycemia makes it difficult to interpret the study properly. As a trial, we performed SPM "Compare-populations: 1 scan/subject (Ancova)" with age as a covariate between the FDG-PET scan of a 76-year-old subject with diabetes mellitus (plasma glucose 145 mg/dl) and mild cognitive impairment, and the 19 normal scans of the present study in SPMgb-, MRIgw-, and Cbll-reference-based analyses (unpublished data). We observed FDG distribution patterns that suggest Alzheimer's disease in the contrast "uptake of the patient < uptake of the normal database" in all reference-based analyses, but increase in the white matter in the contrast "uptake of the patient > uptake of the normal database" was not revealed in any reference-based analyses. The patient was then diagnosed with early Alzheimer's disease.

In conclusion, in the mild hyperglycemic condition, FDG uptake in the SPMgb, MRIgw, and Cbll regions was significantly decreased to 42.7%, 41.3%, and 40.0% of that in the fasting condition. It is noteworthy that FDG distribution patterns in SPMgb- (SPM default) and MRIgw-reference-based analyses were altered under mild hyperglycemia, and the decreased uptake patterns were fairly similar to those observed in Alzheimer's disease. However, when we adopted Cbll as the reference region, the decreased uptake patterns disappeared. We can recommend Cbll-reference-based analysis in the mild hyperglycemic condition to detect decreased uptake patterns. We should pay special attention to controlling the diet condition, monitoring hyperglycemia, and optimizing the reference region in SPM analysis, particularly in the diagnosis of early Alzheimer's disease in clinical FDG-PET.

Acknowledgments The authors are grateful to Drs. Hidenao Fukuyama, Kazuo Hashikawa, and Koichi Ishizu of Kyoto University for proper advice. We thank Drs. Kazunori Kawamura and Takashi Oda for the preparation of FDG and Ms. Miyoko Ando and Ms. Hiroko Tsukinari for nursing. We also thank Dr. Laurence Court for proofreading this manuscript. This research was partially supported by the Grants for Comprehensive Research Project on Longevity Science from the Ministry of Health, Labour and Welfare, Japan.

References

1. Vander Borght T, Laloux P, Maes A, Salmon E, Goethals I, Goldman S. Guidelines for brain radionuclide imaging: perfusion single photon computed tomography (SPECT) using Tc-99m radiopharmaceuticals and brain metabolism positron emission tomography (PET) using F-18 fluorodeoxyglucose. Acta Neurol Belg 2001;101:196–209.
2. Bartenstein P, Asenbaum S, Catafau A, Halldin C, Pilowski L, Pupi K, et al. European Association of Nuclear Medicine procedure guidelines for brain imaging using [^{18}F]FDG. Eur J Nucl Med Mol Imaging 2002;29:43–8.
3. Signorini M, Paulesu E, Friston K, Perani D, Colleluori A, Lucignani G, et al. Rapid assessment of regional cerebral metabolic abnormalities in single subjects with quantitative and nonquantitative [^{18}F]FDG PET: a clinical validation of statistical parametric mapping. Neuroimage 1999;9:63–80.
4. Minoshima S, Frey KA, Koeppe RA, Foster NL, Kuhl DE. A diagnostic approach in Alzheimer's disease using three-dimensional stereotactic surface projections of fluorine-18-FDG PET. J Nucl Med 1995;36:1238–48.
5. Sokoloff L, Reivich M, Kennedy C, Des Rosiers MH, Patlak CS, Pettigrew KD, et al. The [^{14}C]deoxyglucose method for the measurement of local cerebral glucose utilization: theory, procedure, and normal values in the conscious and anesthetized albino rat. J Neurochem 1977;28:897–916.
6. Hasselbalch SG, Knudsen GM, Capaldo B, Postiglione A, Paulson OB. Blood–brain barrier transport and brain metabolism of glucose during acute hyperglycemia in humans. J Clin Endocrinol Metab 2001;86:1986–90.
7. Meyer JH, Gunn RN, Myers R, Grasby PM. Assessment of spatial normalization of PET ligand images using-specific templates. Neuroimage 1999;9:545–53.
8. Benson DF, Kuhl DE, Hawkins RA, Phelps ME, Cummings JL, Tsai SY. The fluorodeoxyglucose 18F scan in Alzheimer's disease and multi-infarct dementia. Arch Neurol 1983;40:711–4.
9. Friedland RP, Brun A, Budinger TF. Pathological and positron emission tomographic correlations in Alzheimer's disease. Lancet 1985;1:228.
10. Duara R, Grady C, Haxby J, Sundaram M, Cutler NR, Heston L, et al. Positron emission tomography in Alzheimer's disease. Neurology 1986;36:879–87.
11. Rapoport SI, Horwitz B, Grady CL, Haxby JV, DeCarli C, Schapiro MB. Abnormal brain glucose metabolism in Alzheimer's disease, as measured by position emission tomography. Adv Exp Med Biol 1991;291:231–48.
12. Fukuyama H, Ogawa M, Yamauchi H, Yamaguchi S, Kimura J, Yonekura Y, et al. Altered cerebral energy metabolism in Alzheimer's disease: a PET study. J Nucl Med 1994;35:1–6.
13. Minoshima S, Foster NL, Kuhl DE. Posterior cingulate cortex in Alzheimer's disease. Lancet 1994;344:895.
14. Minoshima S, Giordani B, Berent S, Frey KA, Foster NL, Kuhl DE. Metabolic reduction in the posterior cingulate cortex in very early Alzheimer's disease. Ann Neurol 1997;42:85–94.
15. Bartlett EJ, Brodie JD, Wolf AP, Christman DR, Laska E, Meissner M. Reproducibility of cerebral glucose metabolic measurements in resting human subjects. J Cereb Blood Flow Metab 1988;8:502–12.
16. Maquet P, Dive D, Salmon E, von Frenckel R, Franck G. Reproducibility of cerebral glucose utilization measured by PET and the [^{18}F]-2-fluoro-2-deoxy-D-glucose method in resting, healthy human subjects. Eur J Nucl Med 1990;16:267–73.
17. Wang GJ, Volkow ND, Overall J, Hitzemann RJ, Pappas N, Pascani K, et al. Reproducibility of regional brain metabolic responses to lorazepam. J Nucl Med 1996;37:1609–13.
18. Tyler JL, Strother SC, Zatorre RJ, Alivisatos B, Worsley KJ, Diksic M, et al. Stability of regional cerebral glucose metabolism in the normal brain measured by positron emission tomography. J Nucl Med 1988;29:631–42.
19. Phelps ME, Huang SC, Hoffman EJ, Selin C, Sokoloff L, Kuhl DE. Tomographic measurement of local cerebral glucose metabolic rate in humans with (F-18)2-fluoro-2-deoxy-D-glucose: validation of method. Ann Neurol 1979;6:371–88.

20. Reivich M, Alavi A, Wolf A, Fowler J, Russell J, Arnett C, et al. Glucose metabolic rate kinetic model parameter determination in humans: the lumped constants and rate constants for [^{18}F]fluorodeoxyglucose and [^{11}C]deoxyglucose. J Cereb Blood Flow Metab 1985;5:179–92.
21. Tataranni PA, Gautier JF, Chen K, Uecker A, Bandy D, Salbe AD, et al. Neuroanatomical correlates of hunger and satiation in humans using positron emission tomography. Proc Natl Acad Sci USA 1999;96:4569–74.
22. Routh VH. Glucose-sensing neurons: are they physiologically relevant? Physiol Behav 2002;76:403–13.
23. Pardridge WM, Boado RJ, Farrell CR. Brain-type glucose transporter (GLUT-1) is selectively localized to the blood–brain barrier: studies with quantitative western blotting and in situ hybridization. J Biol Chem 1990;265:18035–40.
24. Maher F, Vannucci SJ, Simpson IA. Glucose transporter proteins in brain. FASEB J 1994;8:1003–11.
25. Nagamatsu S, Sawa H, Kamada K, Nakamichi Y, Yoshimoto K, Hoshino T. Neuron-specific glucose transporter (NSGT): CNS distribution of GLUT3 rat glucose transporter (RGT3) in rat central neurons. FEBS Lett 1993;334:289–95.
26. Asano T, Katagiri H, Takata K, Tsukuda K, Lin JL, Ishihara H, et al. Characterization of GLUT3 protein expressed in Chinese hamster ovary cells. Biochem J 1992;288:189–93.
27. Yano H, Seino Y, Inagaki N, Hinokio Y, Yamamoto T, Yasuda K, et al. Tissue distribution and species difference of the brain type glucose transporter (GLUT3). Biochem Biophys Res Commun 1991;174:470–7.
28. Ito H. The summary of "Treatment guidelines of diabetes mellitus in the elderly people" drafted by a group of comprehensive research on aging and health (in Japanese). Geriatric Med 1996;34:899–902.